(e,3e) on Helium at Low Impact Energy: The Strongly Correlated Three-Electron Continuum

M. Dürr, A. Dorn, and J. Ullrich

Max-Planck-Institute for Nuclear Physics,

Saupfercheckweg 1, 69117 Heidelberg, Germany

S. P. Cao

(Institute of Modern Physics, Chinese Academy of Science.

Graduate University of Chinese Academy of Science)

A. S. Kheifets

Australian National University, Canberra ACT 0200, Australia

J. R. Götz, J. S. Briggs

University Freiburg, Hermann-Herder-Strasse 3, 79104 Freiburg, Germany

(Dated: November 12, 2006)

Abstract

Double ionization of the helium atom by slow electron impact ($E_0 = 106$ eV) is studied in a kinematically complete experiment. Due to a low excess energy $E_{\rm exc} = 27$ eV above the double ionization threshold, a strongly correlated three-electron continuum is realized. This is demonstrated by measuring and calculating the fully differential cross sections for equal energy sharing of the final state electrons. In the coplanar geometry, these cross sections are dominated by a strong Coulomb repulsion. In a non coplanar geometry, binary collision mechanisms can be identified.

Small systems of Coulomb interacting particles such as the helium atom or the hydrogen molecule have been models for quantum theory since its earliest days. While nearly exact calculations for such systems are available for static, bound state properties, dynamical reactions have proven to be much more difficult to describe theoretically. It was only recently that the dynamics of fundamental three-body systems such as low-energy electron-impact single ionization of atomic hydrogen [1] or photo double ionization of helium [2, 3] could be calculated accurately. Problems still persist for particle impact single ionization of more complex targets than hydrogen as observed even for the most simple multi electron target helium [4]. Experimental and theoretical studies of processes leading to the four-body break-up are still in their infancy. Examples for photon induced reactions are triple ionization of lithium and the complete photo-fragmentation of the deuterium molecule. For the first reaction so far only total cross sections could be measured [5]. For the second reaction fully differential cross sections revealed complex structures in the electron emission pattern [6, 7]. Some key features of these experiments have been reproduced in a recent *ab initio* calculation [8]. In addition, many selection rules for the photo double ionization of molecular hydrogen have been proven [9, 10]. However, because the target nuclei can be taken as fixed, during the time required for the electrons to escape the molecule, the photoionization of the hydrogen molecule is a much-less challenging problem as compared with electron-impact ionization of the helium atom.

In charged particle-atom collisions, double ionization of helium constitutes the most fundamental four-body reaction. Highly differential experiments for this reaction have been performed for different ion species (see e.g. [11, 12]) and for electrons [13, 14]. So far, fully differential studies were restricted to fast electron impact with $E_0 \geq 500$ eV, $v_0 \geq 6$ a.u. In this so-called perturbative regime, the projectile - target interaction is weak and well described by the lowest terms of the Born series. Thus, the reaction can be represented by an effective three-body model involving only the helium fragments. Furthermore, in most collisions the projectile scattering angles and, therefore, the momentum transfers are small and the cross sections very closely resemble these observed in photo-double ionization of helium being governed by the dipole selection rules. For these reasons, various few-body Coulomb methods [15, 16] or the convergent close coupling (CCC) method in combination with the first [17] or second Born approximation [18] were in good agreement with the experimental data on a relative scale.

The full complexity inherent in the four-body dynamics appears only at lower projectile velocities where all the mutual two-body forces involved are of the same magnitude. Particularly interesting is the threshold region where theory predicts that double ionization should proceed via a small subspace of the full many-body configuration space in which the electrons are always at similar distances from the ion and form an equilateral triangle in order to minimize their repulsion [19, 20]. This strongly restricted accessible phase space results in a very small cross section. Therefore, closely above the double ionization threshold $IP = 79$ eV only total cross section measurements exist [21], and this low energy regime is completely unexplored in so far as fully differential measurements are concerned.

In this Letter, we present a combined experimental and theoretical study of the fully differential cross sections for low energy ($E_0 = 106$ eV) electron-impact double ionization of helium. In order to perform these measurements of a cross section of the order of 10^{-20}cm^2, which is about 5% of the maximum cross section for electron impact double ionization at $E_0 = 300$ eV, a newly developed advanced reaction microscope was employed. This apparatus opens the way to the detailed study of break-up reactions close to threshold. Since a large part of the complete phase space of the three final-state electrons carrying the excess energy of $E_{\rm exc} = 27$ eV is covered, detailed insight into the break-up dynamics in the non-perturbative regime is gained.

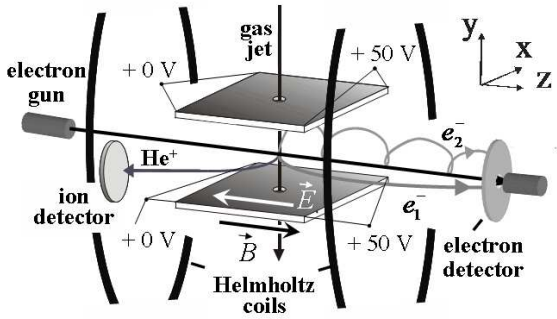

FIG. 1: Scheme of the experimental set-up.

The multi-coincidence multi-electron recoil-ion momentum spectrometer is shown schematically in Fig. 1. A well focused (1 mm), pulsed electron beam (pulse length ≈ 1.5 ns, repetition rate 200 kHz, $\approx 10^4$ electrons/pulse), produced by a standard thermo cathode

gun, crosses and ionizes a supersonic He jet (1 mm diameter, 10^{12} atoms/cm^3). Using parallel electric (1 V/cm) and magnetic (6 G) fields, the fragments in the final state are projected onto 2D position and time sensitive multi-hit channel plate detectors equipped with delay-line read-out. In this way, a large part of the full solid angle is covered, 100% for the detection of target ions and 80% for electrons below 15 eV. From the positions of the hits and the time-of-flight the vector momenta of the particles can be calculated.

In contrast to previous designs [22], in the present reaction microscope the projectile beam (defining the longitudinal direction) is guided exactly parallel to the electric and magnetic extraction fields, requiring a central bore (5 mm diameter) in the forward electron detector to allow for the passage of the non-deflected electrons. It is also to be noted that, due to the jet velocity transversal to the extraction direction, ions have an offset momentum of $p_\perp \approx 6$ a.u. and the ion detector is located off the projectile beam axis. Thus, (i) any projectile beam energy between 30 eV and 2 keV can be realized with the present gun. We aim to reach eV beam energies with meV energy resolution from a photo cathode in the near future. Moreover (ii), scattered projectile electrons with a transverse momentum of 0.2 a.u. $\leq p_\perp \leq$ 1.0 a.u. are detected as well such that, in principle, a quadruple coincidence of all four final state continuum particles can deliver superior background suppression and, due to over-determined kinematics, optimal control by confirming rather than relying on momentum conservation. For the present experiments, as for typical ion-impact data, the recoil-ion momentum resolution is $(\Delta p_\perp, \Delta p_{||}) \approx (0.4, 0.15)$ a.u. For all electrons, including the scattered ones, the transversal resolution is $\Delta p_\perp \leq 0.1$ a.u. The longitudinal resolution for the electrons is $\Delta p_{||} \leq 0.02$ a.u.

The absolute normalization of the (e,3e) cross section has been performed by measuring simultaneously both double and single ionization events and therefore fixing their relative scale. The single ionization data have been normalized on a three-Coulomb wave function (3C) calculation [23]. The accuracy of the absolute cross section obtained by this model was confirmed at a slightly lower energy of $E_0 = 100$ eV using experimental absolute triple differential cross sections published in [24]. In this way the absolute size of the double ionization cross sections can be fixed with an error of $\pm$30%.

In order to demonstrate a strong angular correlation between the three final state continuum electrons, the cross section is plotted in Fig. 2 as a function of their relative emission angles. While θ_{12} is the angle enclosed by the momentum vectors of two arbitrarily chosen

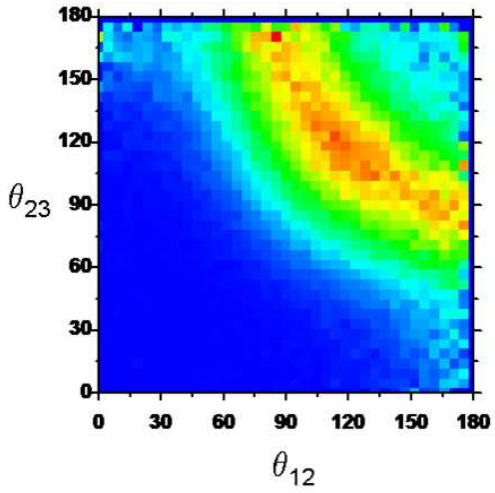

FIG. 2: Cross section differential in the relative emission angle θ_{12} and θ_{23}.

final state electrons e_1 and e_2, θ_{23} is the respective angle enclosed by e_2 and the residual electron e_3. The diagram contains all double ionization events recorded regardless of how the excess energy is shared among the electrons or into which direction the electrons are emitted with respect to the incoming beam. It is clear that the cross section displayed in Fig. 2 reflects a situation far from uncorrelated emission which would have resulted in a uniform and structureless pattern. Electron emission is only allowed along a ridge going from top center to the right center of the diagram (corresponding to emission from a back-to-back configuration of two electrons with the third one emitted perpendicular to the others) to a symmetric configuration where the electron trajectories enclose angles of approximately 120°. Small relative angles $\theta_{12}, \theta_{23} < 90°$ are excluded. The top right region in the diagram corresponds to small angles for $\theta_{13} \leq 360° - \theta_{12} - \theta_{23}$ which are suppressed also. Thus, we are in an energy range where the three continuum electrons are strongly correlated. The threshold regime where, according to theoretical predictions [19, 20], only the symmetric emission should be present with relative angles $\theta_{ij} = 120°$, has not yet apparently been reached in the present experiment. It is important to note that the observed configurations with large relative emission angles imply that the electrons' sum momentum is rather small. Indeed we observe that a large fraction of the projectile momentum k_0= 2.8 a.u. is carried by the residual ion with a high mean longitudinal momentum of $k_R^{||} \approx 2.4$ a.u. Therefore, there must be either a strong momentum transfer to the ion during the collision or double ionization is selective on the large momentum components in the initial state wavefunction.

In the latter case theoretical calculations may become very sensitive to the details of the electronic wavefunction.

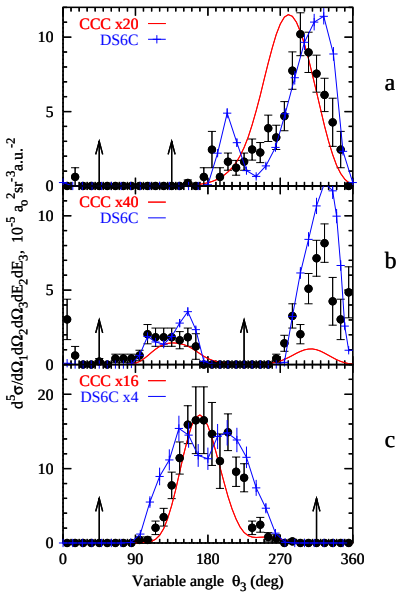

FIG. 3: Fully differential cross sections for equal energy sharing $E_1 = E_2 = E_3 = 9 \pm 3$ eV and the coplanar geometry where the incoming projectile and all outgoing electrons move in a common plane. The cross sections are plotted as a function of θ_3 with respect to the incoming projectile forward direction. The emission angles of the other two electrons are fixed to $\theta_1 = 45°$ and $\theta_2 = 135°$ (a), 225° (b) and 315° (c). Directions of the fixed angle electrons are indicated by arrows. The full width at half maximum of the angular resolution is better than 15°.

In Fig. 3, absolutely normalized, fully differential cross sections are presented for equal energy sharing $E_1 = E_2 = E_3 = 9$ eV and the coplanar scattering geometry where the emitted electrons are ejected in a common plane containing the incoming projectile direction. The cross sections are plotted as a function of one electron emission angle θ_3 with respect to the incoming beam forward direction for fixed emission angle $\theta_1 = 45°$ and three different angles $\theta_2 = 135°$ (a), 225° (b) and 315° (c). Consistent with the cross section pattern in Fig. 2 discussed above, the electron-electron repulsion also dominates emission in the coplanar kinematics with equal energy sharing. For emission angles θ_3 in the vicinity of θ_1 and θ_2 the cross section is vanishing. Furthermore, as can be seen in Fig. 3a and 3c for an angular separation $|\theta_2 - \theta_1| = 90°$, emission of the third electron in between e_1 and e_2 is suppressed (i.e. in the vicinity of 90° and 0°, respectively) and only one broad peak in

the cross section is observed. For the back-to-back emission $|\theta_2 - \theta_1| = 180°$, two relatively narrow maxima with angles around 90° with respect to the fixed electrons direction show up.

Theoretically, emission characteristics of low energy ($E_{\rm exc} = 6$ eV) electron impact double ionization was first studied using a six Coulomb wave function approach (6C) which took into account the interactions of all six two-body subsystems present within the four-particle system [20]. Results of this study indicated the presence of the maxima at the mutual angle values $\theta_{12} = 180°$, $\theta_{23} = 90°$ and $\theta_{12} = 120°$, $\theta_{23} = 120°$ which is consistent with the cross section pattern displayed in Fig. 2. To describe the results of the present study, we employ an improved DS6C final state wave function which is the dynamically-screened variant of the 6C wave function [25]. The DS6C model removes some of the deficiencies of the 6C model since, in contrast to 6C, it accounts for the screening of the two-body potential by the presence of further charged particles.

As an alternative model, we employ the first Born implementation of the CCC method [17] which describes the interaction between the two outgoing electrons exactly whereas the interaction of each of the ejected electrons with the scattered projectile is approximated by the two-body Coulomb density of states, also known as the Gamow factor.

Results of both calculations are presented in Fig. 3 along with the experimental data. In Fig. 3a, the CCC theory predicts only broad peak pointing almost exactly in the direction minimizing the Coulomb repulsion $\theta_3 = 270°$. Conversely, the DS6C calculation shows two maxima. The larger one is situated near the position where the experiment shows its main peak. A smaller peak coincides with a long shoulder towards smaller emission angles seen in the experiment. One should note that the main peak is not located around $\theta_3 = 270°$ which is the preferred direction for the third outgoing electron according to the Coulomb repulsion in this geometry. Rather it is rotated slightly into the forward, incident beam direction (0° or, equivalently, 360°). The explanation of this effect is the memory of the direction of the impinging projectile which breaks the symmetry of the final state. This can be seen explicitly when the different spin-resolved components of the cross section are analyzed [25].

For the back-to-back configuration (Fig. 3b), the angular distance of e_3 relative to the nearest fixed angle electron cannot be larger than 90° and therefore Coulomb repulsion strongly restricts the accessible angular range of θ_3. Both calculations show peak position and width agreeing with the experiment but the relative height of the two peaks is better

reproduced by the DS6C calculation, which shows a split structure in the left peak.

In Fig. 3c, two of the emission angles are fixed symmetrically with respect to the projectile beam direction and therefore the cross section, as a function of θ_3, must be symmetric also with respect to $\theta_3 = 0°$ and 180°. The CCC theory agrees well with the experiment concerning the shape whereas the DS6C calculation displays a double-peak structure which is not clearly discernible in the experiment due to large error bars. On the other hand for the geometries shown the absolute size of the CCC calculation is wrong by one to two orders of magnitude. This not surprising considering the crude approxiamtions involved in this model. The absolute magnitude of the cross section is much better reproduced by the DS6C calculation. Only in Fig. 3c, there is a considerable deviation from experiment.

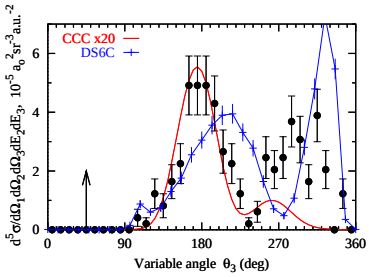

FIG. 4: As Fig. 3 but with the emission angle of electron e_2 fixed perpendicular to the plane containing the incoming beam and the outgoing electrons e_1 and e_3.

Finally, in Fig. 4 we show a geometry where one of the electron momentum vectors is fixed again at $\theta_1 = 45°$ but the second electron e_2 is emitted perpendicular to the plane containing the incoming beam and the other two electrons. Thus, the electron repulsion between electron e_2 and the two other electrons is constant for all in-plane angles. In this configuration, the angular emission pattern of electron e_3 is only influenced by the final state interaction with electron e_1. Consequently, the cross section shows more structure with a broad peak at 180° and a second peak around 300°. This cross section pattern can be interpreted as a remnant of the binary/recoil lobe structure observed for (e,2e) collisions. If one of the electrons, fixed at $\theta_1 = 45°$, is considered as the scattered projectile then the maximum at 300° points roughly along the momentum transfer direction as is characteristic for the binary lobe. The second peak would correspond to the recoil lobe which is typically observed close to 180° (see, e.g. [23]). Both peaks are not aligned perfectly along the momentum transfer axis as it is the case for fast charged particle impact but are shifted

away from the scattered projectile direction due to the final state repulsion. The CCC calculation describes the shape of the 180° peak almost exactly but the relative hight of the 290° peak is far too small. In the DS6C calculation, the relative strengths of the peaks is just the opposite.

In conclusion, we have investigated, both experimentally and theoretically, the (e,3e) reaction on He at low excess energy. The inspection of the global emission characteristics of the three outgoing electrons, reveals their strongly correlated motion in the final state. Besides the equilateral triangle configuration predicted by threshold theory [19] and resulting in emission with 120° relative angles also the back-to-back configuration of two electrons with the third one being emitted perpendicular to the others is observed. In a recent classical calculation [26], this configuration was predicted to dominate the three electron escape even below 1 eV excess energy. Choosing equal energy sharing an ideal three electron continuum state is realized where the electrons are indistinguishable. Fully differential cross section in the coplanar geometry where the emission angles of two electrons are fixed are non-vanishing only if the variable angle electron is emitted in the direction minimizing the Coulomb repulsion and forming an almost symmetric configuration with respect to the two other electrons. This emission pattern is predicted by a CCC calculation in which the projectile-target interaction is treated in the first Born approximation. The Coulomb interaction of the two ejected electrons is included in full whereas the interaction of these electrons with the scattered projectile in the final state is approximated by the Gamow factor. The fact that such a crude approximation works fairly well tells us that the dominant factor which determines the emission pattern is the strong Coulomb repulsion in the final state. On the other hand the absolute magnitude of the cross section cannot be reproduced. A more sophisticated treatment of the full 4-body Coulomb problem within the DS6C method shows better agreement concerning both, the relative and the absolute peak heights. It also exhibits a richer structure of the cross section with distinct peaks, which are not entirely seen in the experiment. Increasing the accuracy of the cross section measurement and reducing the experimental error bars would confirm, or otherwise, these structures.

The Heidelberg team thanks R. Moshammer for fruitful discussions and A. Czasch for helpful support with the event-reconstruction in the data analysis. ASK wishes to thank

MPI-Heidelberg for hospitality.

[1] C. W. McCurdy, M. Baertschy, and T. N. Rescigno, J. Phys. B **37**, R137 (2004).

[2] J. S. Briggs and V. Schmidt, J. Phys. B **33**, R1 (2000).

[3] L. Avaldi and A. Huetz, J. Phys. B **38**, S861 (2005).

[4] D.H. Madison, D. Fischer, M. Foster, M. Schulz, R. Moshammer, S. Jones, and J. Ullrich, Phys. Rev. Lett. **91**, 253201-1 (2003).

[5] R. Wehlitz, T. Pattard, M. T. Huang, I. A. Sellin, J. Burgdörfer, and Y. Azuma, Phys. Rev. A **60**, 030704 (2000).

[6] T. Weber, A. Czasch, O. Jagutzki, A. Müller, V. Mergel, A. Kheifets, E. Rothenberg, G. Meigs, M. Prior, S. Daveau, et al., Nature **431**, 437 (2004).

[7] M. Gisselbrecht, M. Lavollee, A. Huetz, P. Bolognesi, L. Avaldi, D. P. Seccombe, and T. J. Reddish, Phys. Rev. Lett. **96**, 153002 (2006).

[8] W. Vanroose, F. Martin, T. N. Rescigno, and C. W. McCurdy, Science **310**, 1787 (2005).

[9] M. Walter, A. V. Meremianin, and J. S. Briggs, J. Phys. B **36**, 4561 (2003).

[10] M. Walter, A. Meremianin, and J. S. Briggs, Phys. Rev. Lett. **90**, 233001 (2003).

[11] D. Fischer, R. Moshammer, A. Dorn, J. R. C. López-Urrutia, B. Feuerstein, C. Höhr, C. D. Schröter, S. Hagmann, H. Kollmus, R. Mann, et al., Phys. Rev. Lett. **90**, 243201 (2003).

[12] M. Schulz, D. Fischer, R. Moshammer,and J. Ullrich, J. Phys. B **38**, 1363 (2005).

[13] A. Dorn, A. Kheifets, C. D. Schröter, B. Najjari, C. Höhr, R. Moshammer,and J. Ullrich, Phys. Rev. Lett. **86**, 3755 (2000).

[14] I. Taouil, A. Lahmam-Bennani, A. Duguet, M. Lecas, and L. Avaldi, Phys. Rev. Lett. **81**, 4600 (1998).

[15] A. Lahmam-Bennani, I. Taouil, A. Duguet, M. Lecas, L. Avaldi, and J. Berakdar, Phys. Rev. A **59**, 3548 (1999).

[16] J. R. Götz, M. Walter, and J. S. Briggs, J. Phys. B **38**, 1569 (2005).

[17] A. S. Kheifets, I. Bray, A. Duguet, A. Lahmam-Bennani, and I. Taouil, J. Phys. B **32**, 5047 (1999).

[18] A. S. Kheifets, Phys. Rev. A **69**, 032712 (2004).

[19] H. Klar and W. Schlecht, J. Phys. B **9**, 1699 (1976).

[20] A. W. Malcherek and J. S. Briggs, J. Phys. B **30**, 4419 (1997).

[21] S. Denifl, B. Gstir, G. Hanel, L. Feketeova, S. Matejcik, K. Becker, A. Stamatovic, P. Scheier, and T. D. Märk, J. Phys. B **35**, 4685 (2002).

[22] J. Ullrich, R. Moshammer, A. Dorn, R. Dörner, L. P. H. Schmidt, and H. Schmidt-Böcking, Rep. Prog. Phys. **66**, 1463 (2003).

[23] M. Dürr, C. Dimopoulou, A. Dorn, B. Najjari, I. Bray, D. V. Fursa, Z. Chen, D. H. Madison, K. Bartschat, and J. Ullrich, J. Phys. B **39**, 4097 (2006).

[24] I. Bray and D. V. Fursa, Phys. Rev. Lett. **76**, 2674 (1996).

[25] J. R. Götz, M. Walter, and J. S. Briggs, J. Phys. B **39**, 4365 (2006).

[26] A. Emmanouilidou and J. M. Rost, J. Phys. B **39**, 4037 (2006).